JOURNAL OF GUIDANCE, CONTROL, AND DYNAMICS
Vol. 26, No. 2, March–April 2003

New Interceptor Guidance Law Integrating Time-Varying and Estimation-Delay Models

Tal Shima,* Josef Shinar,† and Haim Weiss‡
Technion—Israel Institute of Technology, 32000 Haifa, Israel

The paper presents a synthesis of a new guidance law, derived using differential games concepts, for the interception of highly maneuvering targets. The synthesis is based on the integration of two recently demonstrated improvement features: namely, the use of a time-varying linear kinematics game model and the compensation of the inherent estimation delay of the target acceleration. The new guidance law is implemented in a generic yet realistic noise-corrupted three-dimensional nonlinear ballistic missile defense scenario by using a suitable three-dimensional estimator. The test against worst-case target maneuvers demonstrates a significant improvement compared to other known guidance laws indicating a potential breakthrough in interceptor guidance.

I. Introduction

HISTORICALLY, the typical target of interceptor missiles has been a manned aircraft, against which the missile had substantial advantage in speed, maneuverability, and agility. Moreover, miss distances of a few meters, compatible with the lethal radius of the missile warhead, were considered admissible. Because of these facts, even a simple guidance law such as proportional navigation (PN) could guarantee the target destruction. The Gulf War introduced the tactical ballistic missile (TBM), able to carry nonconventional warheads, as a new type of target. Successful interception of a TBM, much less vulnerable than an aircraft, requires a very small miss distance or even a direct hit. Several ballistic missile defense systems are currently in development. Because of advances in technology, these systems (such as ARROW and PAC-3) succeeded to demonstrate, using conventional guidance concepts, excellent homing accuracy against such nonmaneuvering targets.[1,2]

Although known TBMs were not designed to maneuver because of their high reentry speed, they have a substantial maneuverability potential in the atmosphere. Moreover, this potential can be made applicable by a modest technical effort. The same is true for future high-speed antiship or cruise missiles. Paradoxically, the successful current development of ballistic missile defense systems can serve to motivate the future development of maneuverable antisurface missiles. Against such threats interceptor missiles will have only a marginal maneuverability advantage. Hence, the required small miss distances are not achievable by using conventional guidance laws even in a noise-free environment, as it was demonstrated by recent simulation studies.[3,4]

Most missile guidance laws used at the present, including PN, were derived using a linear quadratic optimal control formulation assuming perfect information.[5] Such a formulation requires an assumption on the future evolution of the target maneuver. If this assumption is correct (and the lateral acceleration of the interceptor does not saturate), such a guidance law can reduce the miss distance to zero. However, if this assumption is wrong very large miss distances are created. Because target maneuvers are independently controlled, the optimal control formulation is obviously deficient. The interception of a maneuverable target has to be formulated as a zero-sum pursuit–evasion game. By using such a formulation, the engagement between two objects with ideal dynamics, constant velocities, and constant bounds on the lateral accelerations was investigated by Gutman and Leitmann.[6] This scenario model was later extended to include first-order pursuer dynamics[7] and similar evader dynamics[8] leading to a guidance law denoted as DGL/1.

The assumption of constant speeds and fixed maneuverability boundaries, used as a part of linear guidance dynamics, is often unsuitable for realistic interception scenarios. Gazit and Gutman[9] developed a guidance law for a pursuer with a constant acceleration, using a time-varying linear model assuming for both players ideal dynamics and constant bounded controls. In a recent paper[10] a time-varying linear game model with bounded controls has been used for deriving a new guidance law for an interception scenario between two missiles with first-order dynamics and known time-varying velocities and lateral acceleration bounds. It was demonstrated that this guidance law, denoted as DGL/E, provides improved homing accuracy in a typical TBM interception scenario.

The perfect information formulation of an interception scenario in general, and a ballistic missile defense (BMD) scenario in particular, is not realistic. The information structure in a BMD scenario is imperfect and also asymmetrical. The ballistic missile will probably have no information on the relative state of the interceptor or even on its existence, whereas the interceptor obtains noise-corrupted measurements on the relative position of its target. To make the task of the interceptor not trivial, it is expected that such a blind target will maneuver randomly. The interceptor needs to use an estimator in order to filter the measurement noise and to estimate the state variables necessary for the implementation of the guidance law. In modern guidance laws one of these variables is the target acceleration, which cannot be measured directly. The underlying assumption in a filter's design is that the mathematical and statistical model of the system is perfectly known. Inaccuracy of the system model can result in serious performance degradation. The simplest model uses a zero mean white noise to represent the target acceleration uncertainty.[11] Singer[12] used a more realistic model which assumes that the target acceleration is a Poisson-distributed random process with piecewise constant acceleration. In this paper a first-order linear system excited by white noise, having the same exponential autocorrelation function (denoted as ECA—exponentially correlated acceleration) as the piecewise constant Singer model, is used for the estimator design. The technique of replacing the original system and the random input (the target maneuver) by an augmented system excited only by a white noise is denoted as the shaping filter (SF) method.[13] The augmented system, composed of the original system and a SF, has an output with the same first- and second-order statistics as the original system.

Presented as Paper 2001-4344 at the AIAA Guidance, Control, and Navigation Conference, Montreal, Canada, 6–9 August 2001; received 14 February 2002; revision received 12 August 2002; accepted for publication 27 August 2002.

*Doctoral Student, Faculty of Aerospace Engineering; currently System Engineer, RAFAEL Armament Development Authority, Ltd., P.O. Box 2250, Department 35, Haifa 31021, Israel; shima_tal@yahoo.com. Member AIAA.

†Professor Emeritus, Faculty of Aerospace Engineering; aer4301@aerodyne.technion.ac.il. Fellow AIAA.

‡Lady Davis Visiting Scientist, Faculty of Aerospace Engineering; currently Research Fellow, RAFAEL Armament Development Authority, Ltd., P.O. Box 2250, Department 35, Haifa 31021, Israel; haimw@rafael.co.il. Member AIAA.

Implementing the optimal pursuer strategy of the perfect information game as the interceptor's guidance law with a typical estimator yields very disappointing results. The miss distance is never zero, and there is a high sensitivity to the structure of the (unknown) target maneuver.[14] The poor performance can be attributed to the unjustified reliance on the certainty equivalence property.[15] This property states that the optimal control law for a stochastic control problem is the optimal control law for the associated deterministic (certainty equivalent) problem. The validity of the certainty equivalence property was proved for linear quadratic Gaussian optimal control problems with unbounded control; the proof was based on assuming a strictly classical information pattern, where all of the past outputs and controls are available at any time. For such problems the estimator and the controller can be designed separately, and the estimated states should be used in the control law of the deterministic problem.

The certainty equivalence property has never been proved for realistic missile guidance problems, characterized by bounded control, non-Gaussian random target maneuvers and saturated state variables. Nevertheless, it has been of common practice in the guided missile community to assume certainty equivalence when designing the interceptor's control law. The approach taken in this paper is different; it is based on the suggestion of Witsenhausen[15] that states if the validity of the certainty equivalence cannot be proven then the estimator can still be designed independently of the controller, but the optimal control depends on the conditional probability density function resulting from the estimation process.

In previous works[14,16] a simplified model, where the only imperfection in the estimation process is a pure time delay in the estimation of the target acceleration, was used. Based on this model, a guidance law, denoted as DGL/C, compensating for this delay was derived.[16] It was demonstrated in a two-dimensional linearized interception scenario that the use of DGL/C guarantees smaller "worst-case" miss distances than other guidance laws used in earlier studies.

The objective of this paper, as well as its contribution to missile guidance theory and to the challenging task of ballistic missile defense, is the presentation of the synthesis of a new guidance law by integrating the features of a time-varying game model[10] and the compensation of the estimation delay.[16] This guidance law, developed by using deterministic two-dimensional linear models and denoted as DGL/EC, is implemented in two orthogonal guidance channels using the three-dimensional estimator of Ref. 17 and tested in a realistic three-dimensional nonlinear noise-corrupted interception scenario.

In the next section the interception scenario of a maneuvering antisurface missile is formulated as a zero-sum pursuit–evasion game of imperfect information. The solution of the perfect information version of this game using a time-varying linear model is briefly repeated in Sec. III. In Sec. IV the formulation of the imperfect information engagement as a delayed information game and its solution yielding a new guidance law are presented. The outline of a suitable three-dimensional estimator for implementing this guidance law is described in Sec. V. The integrated estimator–guidance algorithm is tested in Sec. VI in a realistic three-dimensional nonlinear noise-corrupted interception scenario. Conclusions are offered in the last section.

II. Problem Outline

The investigated interception scenario is the end game between an interceptor missile launched against a maneuverable antisurface missile. As an example, a reentering TBM of high maneuverability is chosen. The scenario is characterized by a near head-on engagement of high velocity with variable altitude. Typical velocity and maneuverability profiles of both missiles are shown in Figs. 1 and 2.

In the investigated interception scenario (with a closing velocity of approximately 5.5 km/s) the following assumptions (some of them based on an earlier study[3]) are made:

1) The relative end-game trajectory can be linearized around a fixed reference line such as the initial line of sight.

2) The velocity profiles of both missiles on a nominal trajectory are known and can be expressed as the function of time.

3) The maximum lateral acceleration of each missile on a nominal trajectory is known as a function of time.

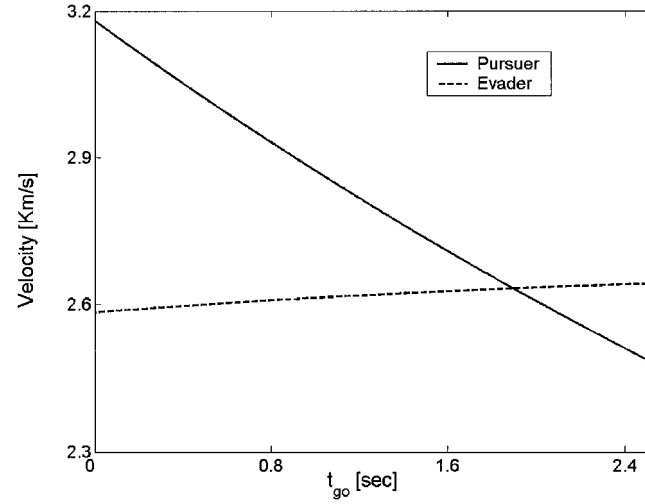

Fig. 1 End-game velocity profiles.

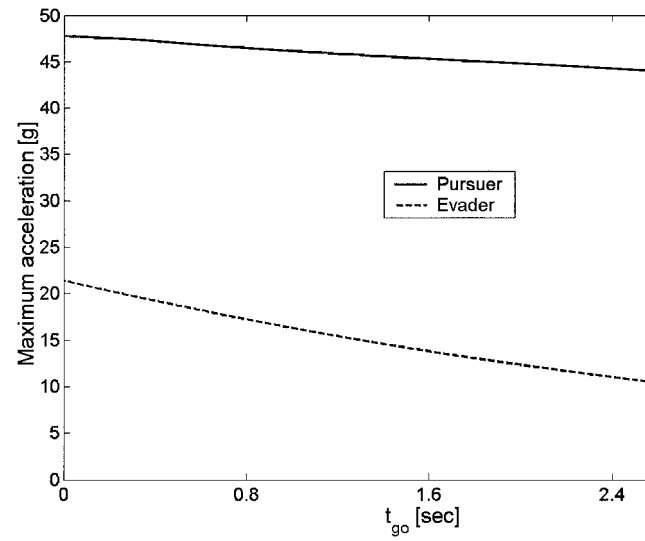

Fig. 2 End-game maneuverability profiles.

4) Both missiles can be represented by point–mass models with linear control dynamics.

5) The maneuvering dynamics of the interceptor and target can be approximated by first-order transfer functions with time constants τ_P and τ_E, respectively.

6) The target has no information on the state of the interceptor.

7) The interceptor has noisy measurements of the target's relative position.

In the sequel this end game is formulated as a zero-sum pursuit–evasion game. The pursuer is the interceptor missile, and the maneuvering target is the evader.

III. Perfect Information Three-Dimensional Game

The analysis in this section is based on the assumption that both players have perfect information on the state variables and the parameters of the game.

A. Reduction to Two-Dimensional Problem

The three-dimensional application of the PN guidance law has been presented by Adler.[18] Assuming small deviations from a collision course, the nonlinear vector equations were linearized yielding two independent linear differential equations of identical form in perpendicular planes. Based on this decomposition, PN has been implemented in cruciform missiles using two independent perpendicular guidance channels. In spite of this simplification, this practice has proved itself in a wide range of applications. Hence, in the derivation of the guidance law presented herein only one plane of the interception scenario is analyzed.

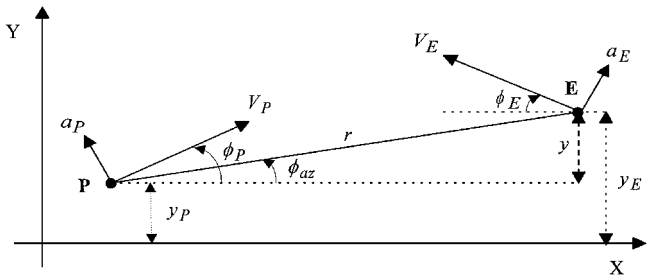

Fig. 3 Planar end-game geometry.

B. Linearized Two-Dimensional Game Model

In Fig. 3 a schematic view of the planar end-game geometry is shown, where the X axis is aligned with the initial line of sight, r is the range between the missiles, and ϕ_{az} is the angle between the current and initial line of sight. The respective velocity vectors are generally not aligned with the reference line. The angles ϕ_p and ϕ_E are, however, small. Thus, the approximations $\cos(\phi_i) \approx 1$, $\sin(\phi_i) \approx \phi_i$, $(i = P, E)$ are uniformly valid and coherent with assumption (1). Nevertheless, the longitudinal accelerations of each missile can have nonnegligible components normal to the line of sight.

Based on assumptions (1) and (2), the final time t_f of the interception can be computed for any given initial conditions of the end game solving

$$t_f = \arg\left\{ \mathrm{X_f} = \mathrm{X_0} - \int_{t_0}^{t_f} [V_E(t) + V_P(t)]\,\mathrm{d}t = 0 \right\} \tag{1}$$

where $\mathrm{X_0}$ and $\mathrm{X_f}$ are the evader positions relative to the pursuer along the X axis at times t_0 and t_f, respectively. If $\mathrm{X_0}$ is known, the time-to-go can be calculated based on Eq. (1) as

$$t_{\mathrm{go}} = t_f - t \tag{2}$$

The state vector associated with the linearized relative motion normal to the reference line is

$$\boldsymbol{X} = [y, \dot{y}, a_P, a_E, \phi_P, \phi_E]^T \tag{3}$$

where

$$y = y_E - y_P \tag{4}$$

From the known velocity profiles $V_P(t)$ and $V_E(t)$ the respective longitudinal accelerations $a_{\mathrm{xP}}(t)$ and $a_{\mathrm{xE}}(t)$ can be computed and substituted into the equations of motion, which can be written in the form

$$\dot{\boldsymbol{X}} = \boldsymbol{A}(t)\boldsymbol{X} + \boldsymbol{B}(t)u + \boldsymbol{C}(t)v, \qquad \boldsymbol{X}(0) = \boldsymbol{X}_0 \tag{5}$$

where

$$\boldsymbol{A}(t) = \begin{bmatrix} 0 & 1 & 0 & 0 & 0 & 0 \\ 0 & 0 & -1 & 1 & -a_{\mathrm{xP}}(t) & a_{\mathrm{xE}}(t) \\ 0 & 0 & -1/\tau_P & 0 & 0 & 0 \\ 0 & 0 & 0 & -1/\tau_E & 0 & 0 \\ 0 & 0 & 1/V_p(t) & 0 & 0 & 0 \\ 0 & 0 & 0 & 1/V_E(t) & 0 & 0 \end{bmatrix} \tag{6}$$

$$\boldsymbol{B}(t) = \begin{bmatrix} 0 & 0 & a_P^{\max}(t)/\tau_P & 0 & 0 & 0 \end{bmatrix}^T \tag{7}$$

$$\boldsymbol{C}(t) = \begin{bmatrix} 0 & 0 & 0 & a_E^{\max}(t)/\tau_E & 0 & 0 \end{bmatrix}^T \tag{8}$$

$$u = a_p^c / a_p^{\max}(t), \qquad |u| \le 1 \tag{9}$$

$$v = a_E^c / a_E^{\max}(t), \qquad |v| \le 1 \tag{10}$$

and a_P^c and a_E^c are the commanded lateral accelerations of the pursuer and evader, respectively; the maximum available values of these accelerations can be expressed as a function of time as $a_P^{\max}(t)$ and $a_E^{\max}(t)$, respectively.

The natural cost function of the perfect information game is the miss distance

$$J = |\boldsymbol{D}\boldsymbol{X}(t_f)| = |x_1(t_f)| \tag{11}$$

where

$$\boldsymbol{D} = (1, 0, 0, 0, 0, 0) \tag{12}$$

The pursuer, applying u, wants to minimize Eq. (11), whereas the evader, applying v, wants to maximize it.

C. Transformation to Scalar Problem

To reduce the order of the problem, the following transformation is introduced[7]:

$$Z(t) = \boldsymbol{D}\boldsymbol{\Phi}(t_f, t)\boldsymbol{X}(t) \tag{13}$$

where $\Phi(t_f, t)$ is the transition matrix of the original homogeneous system. The new scalar state variable $Z(t)$ has the physical interpretation of the zero-effort miss distance (ZEM). The ZEM is obtained when both players use zero control from the current time until the end of the interception.

The transformation (13) reduces the vector equation (5) to a scalar dynamic equation of the form

$$\dot{Z}(t) = B(t_f, t)u + C(t_f, t)v \tag{14}$$

where

$$B(t_f, t) = \boldsymbol{D}\boldsymbol{\Phi}(t_f, t)\boldsymbol{B}(t) \tag{15}$$

and

$$C(t_f, t) = \boldsymbol{D}\boldsymbol{\Phi}(t_f, t)\boldsymbol{C}(t) \tag{16}$$

The cost function expression given in Eq. (11) is replaced by

$$J = |Z(t_f)| \tag{17}$$

and has to be minimized by the pursuer and maximized by the evader.

Using the homogeneous solution of Eq. (5), the ZEM of the problem is

$$Z(t) = Z_{\mathrm{PN}}(t) - \Delta Z_{a_p}(t) + \Delta Z_{a_E}(t) - \Delta Z_{\phi_p}(t) + \Delta Z_{\phi_E}(t) \tag{18}$$

where (for details, see Ref. 10)

$$Z_{\mathrm{PN}}(t) = x_1(t) + x_2(t)t_{\mathrm{go}} \tag{19}$$

$$\Delta Z_{a_P}(t) = x_3(t)\tau_P^2[\psi(t_{\mathrm{go}}/\tau_P) + \mathrm{III}_P(t_f, t)] \tag{20}$$

$$\Delta Z_{a_E}(t) = x_4(t)\tau_E^2 \cdot [\psi(t_{\mathrm{go}}/\tau_E) + \mathrm{III}_E(t_f, t)] \tag{21}$$

$$\Delta Z_{\phi_P}(t) = x_5(t)\lfloor \mathrm{IV}_P(t_f, t) - V_P(t)t_{\mathrm{go}} \rfloor \tag{22}$$

$$\Delta Z_{\phi_E}(t) = x_6(t)\lfloor \mathrm{IV}_E(t_f, t) - V_E(t)t_{\mathrm{go}} \rfloor \tag{23}$$

and

$$\mathrm{III}_i(t_f, t) \triangleq \frac{1}{\tau_i^2}\int_t^{t_f}\int_\zeta^{t_f} a_{\mathrm{xi}}(\xi)\int_\xi^{t_f} \frac{e^{-\varsigma/\tau_i}}{V_i(\varsigma)}\,\mathrm{d}\varsigma\,\mathrm{d}\xi\,\mathrm{d}\zeta, \qquad i = P, E \tag{24}$$

$$\mathrm{IV}_i(t_f, t) \triangleq \int_t^{t_f} V_i(\zeta)\,\mathrm{d}\zeta, \qquad i = P, E \tag{25}$$

Note that

$$\psi(\zeta) = e^{-\zeta} + \zeta - 1 \ge 0 \quad \forall \quad \zeta > 0 \tag{26}$$

The integrals of Eq. (24) have an analytic form only for very special cases of $V_P(t)$ and $V_E(t)$. In general, they have to be computed numerically.

The time derivative of Eq. (18) takes the form of Eq. (14), where

$$B(t_f, t) = -a_P^{\max}(t)[\psi(t_{\mathrm{go}}/\tau_P) + \mathrm{III}_P(t_f, t)]\tau_P \tag{27}$$

$$C(t_f, t) = a_E^{\max}(t)[\psi(t_{\mathrm{go}}/\tau_E) + \mathrm{III}_E(t_f, t)]\tau_E \tag{28}$$

D. Solution of Two-Dimensional Game

The perfect information linear zero-sum differential game with bounded controls, formulated by Eqs. (14–17), is solved in this section in the most general form.

The Hamiltonian of the game is

$$H = \lambda_z[B(t_f, t)u + C(t_f, t)v] \tag{29}$$

where λ_z is the costate variable satisfying

$$\dot{\lambda}_z = -\frac{\partial H}{\partial Z} = 0 \tag{30}$$

$$\lambda_z(t_f) = \left.\frac{\partial J}{\partial Z}\right|_{t_f} = \text{sign}\{Z(t_f)\}, \qquad Z(t_f) \neq 0 \tag{31}$$

meaning that

$$\lambda_z(t) = \text{sign}\{Z(t_f)\}, \qquad Z(t_f) \neq 0 \tag{32}$$

as long as $\lambda_z(t)$ is continuous. This allows determining the optimal strategies as

$$u^* = \arg\min H = -\text{sign}\{B(t_f, t)Z(t_f)\}, \qquad Z(t_f) \neq 0 \tag{33}$$

$$v^* = \arg\max H = \text{sign}\{C(t_f, t)Z(t_f)\}, \qquad Z(t_f) \neq 0 \tag{34}$$

Assuming that $B(t_f, t) < 0$ and $C(t_f, t) > 0$, the optimal strategies become

$$u^* = v^* = \text{sign}\{Z(t_f)\}, \qquad Z(t_f) \neq 0 \tag{35}$$

Substitution of Eq. (35) into Eq. (14) yields the optimal game dynamics

$$\dot{Z}^* = \Gamma(t_f, t)\text{sign}\{Z(t_f)\}, \qquad Z(t_f) \neq 0 \tag{36}$$

with

$$\Gamma(t_f, t) = [B(t_f, t) + C(t_f, t)] \tag{37}$$

Integrating Eq. (36) backward from any end condition $Z(t_f)$ generates candidate optimal trajectories leading to the eventual decomposition of the game space. In a recent paper[10] five different (scenario parameters dependent) examples were reviewed. Here only one case, where $\Gamma(t_f, t)$ changes its sign once, is presented in Fig. 4.

As it can be seen, the optimal trajectories have an extremum at $t_{go} = (t_{go})_s$, which is the solution of $\Gamma(t_f, t) = 0$. If a backwards-generated candidate optimal trajectory intersects the $Z = 0$ axis, it ceases to be optimal because of the change in sign$\{Z\}$. The two families of such trajectories define a dispersal line of the game dominated by the evader (on the dispersal line $u^* = 0$ and $v^* = \pm 1$). The pair

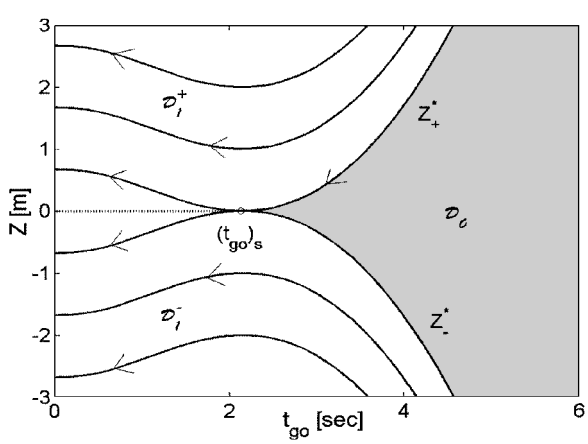

Fig. 4 Example of game space decomposition.

of optimal trajectories Z_+^* and Z_-^* that reach the $Z = 0$ axis tangentially at $t_{go} = (t_{go})_s$ are the boundary trajectories between the two regions of the different game solutions

$$\mathcal{D}_1 = \left\{(Z, t_{go}): |Z(t_{go})| \geq Z_+^*(t_{go}) \cup (t_{go})_s \geq t_{go} \geq 0\right\} \tag{38}$$

$$\mathcal{D}_0 = \left\{(Z, t_{go}): |Z(t_{go})| < Z_+^*(t_{go}) \cap t_{go} > (t_{go})_s\right\} \tag{39}$$

In $\mathcal{D}_1$ the optimal strategies (35) can be expressed in a state feedback form

$$u^* = v^* = \text{sign}\{Z\} \quad \forall \quad Z \neq 0 \tag{40}$$

and the value of the game is a function of the initial conditions

$$J^*(Z_0, t_0) = |Z_0| + \int_{t_0}^{t_f} \Gamma(t_f, t)\,\mathrm{d}t \tag{41}$$

In $\mathcal{D}_0$ the optimal strategies are arbitrary. Every trajectory that starts in this region must go through the "throat" $(Z, t_{go}) = [0, (t_{go})_s]$. Consequently, the value of the game in this entire region is constant:

$$J_0^*(Z_0, t_0) = \int_{t_s}^{t_f} \Gamma(t_f, t)\,\mathrm{d}t \tag{42}$$

The boundary trajectories and the dispersal line $\{Z(t_{go}) = 0$ for $(t_{go})_s \geq t_{go} \geq 0\}$, dominated by the evader, belong to $\mathcal{D}_1$. The dispersal line separates $\mathcal{D}_1$ into two subregions denoted as $\mathcal{D}_1^+$ and $\mathcal{D}_1^-$.

Remark: If $\Gamma(t_f, t) < 0$ for all $t_{go} > 0$, both $(t_{go})_s$ and J_0^* are zero, indicating a most desired guaranteed "hit-to-kill" homing performance, in the ideal perfect information case.

IV. Imperfect Information Three-Dimensional Game

In this section the assumption of perfect information is removed. The relevant assumptions about the information structure are given by assumptions (6) and (7) in Sec. II.

A. Maneuver Strategies

In the realistic version of the problem, the blind target cannot implement a deterministic optimal strategy becasue of the lack of information. The target designer's obvious objective is to avoid interception, in spite of the lack of information, allowing the target to hit its designated surface target. Not maneuvering, or even performing a constant maneuver, generates predictable trajectories, leading to a successful intercept. Thus, the target must maneuver randomly. Based on the perfect information game solution, outlined in the preceding section, and optimal avoidance analysis,[19,20] the optimal target maneuver sequence has a bang–bang structure (40). Implementation of such a random strategy over the short duration of the end game consists of a maximal maneuver command in one direction, followed by a maximal maneuver command in the opposite direction at a randomly selected time t_{sw}.

Implementation of the different guidance laws requires the knowledge of the zero-effort miss distance; thus, the scenario's state variables are needed. Some of these variables have to be estimated based on noisy measurements. In the sequel the guidance law is derived based on a model of the estimator; in its implementation the estimated states are used.

B. Estimator Modeling

As in earlier investigations,[14,16] in the current work a simplified model for the estimation process is used; in the model the only estimation process imperfection is a pure time delay Δt_{est} in estimating the target acceleration a_E. Accordingly, the observation vector of the pursuer is given by

$$z_i(t) = x_i(t), \qquad i = 1, 2, 3, 5, 6$$

$$z_4(t) = a_E(t - \Delta t_{est}) \tag{43}$$

The inherent delay in estimating the target acceleration results from the time needed to detect (identify) a maneuver. In Ref. 21 an approximation of the detection time has been computed. The computation

is based on the assumption that a target maneuver can be detected when the absolute value of the measured deviation of the target position from its nominal trajectory exceeds twice the value of the standard deviation of the respective measurement noise. The deviation in the position of a missile with first-order dynamics, caused by a lateral acceleration step command change of magnitude Δa_E^c at $t = 0$, can be approximated by

$$\Delta y(t) \cong \frac{\Delta a_E^c t^3}{6\tau_E} \tag{44}$$

Hence, the minimal detection time can be approximated by

$$T_{\mathrm{id}}^{\min} \cong \arg_t\{\Delta y(t) = 2\sigma_y = 2r\sigma_a\} \cong \sqrt[3]{\frac{12\tau_E r\sigma_a}{\Delta a_E^c}} \tag{45}$$

where σ_y is the standard deviation of the measurement noise of $y(t)$ and σ_a is the corresponding angular standard deviation.

As can be observed from Eq. (45), $T_{\mathrm{id}}^{\min}$ is range dependent. In this paper Δt_{est} was assumed constant, and its value was chosen, as described in the sequel, using a minmax search for the delay that provides the best homing performance.

C. New Problem Formulation

The deterministic model of the estimator, given in Eq. (43), leads to the reformulation of the interception scenario of a maneuvering antisurface missile as a delayed information zero-sum pursuit–evasion game. This formulation allows solving the game without a stochastic analysis. Given the dynamic system (5–8) and a set of initial conditions, the objective is to minimize the supremum (taken over the evader's control) of the cost function (11), subject to the available measurements of Eq. (43). For a worst-case analysis it is also assumed that the evader has perfect knowledge of all of the state variables and the delay of the pursuer.

Because of the estimation delay, one observes the delayed value of Z instead of its actual value; this estimated value of $Z(t)$ is

$$Z_{\mathrm{est}}(t) = Z_{\mathrm{PN}}(t) - \Delta Z_{a_p}(t) - \Delta Z_{\phi_p}(t) + \Delta Z_{\phi_E}(t) + \left\{\Delta Z_{a_E}(t)\right\}_{\mathrm{est}} \tag{46}$$

where

$$\left\{\Delta Z_{a_E}(t)\right\}_{\mathrm{est}} = \tau_E^2[\psi(t_{\mathrm{go}}/\tau_E) + \mathrm{III}_E(t_f, t)]x_4(t - \Delta t_{\mathrm{est}}) \tag{47}$$

and the other terms are given by Eqs. (19), (20), (22), and (23), respectively.

Given the delayed measurement $x_4(t - \Delta t_{\mathrm{est}})$, the uncertainty in the true value of $\Delta Z_E(t)$ is bounded by

$$\left[\Delta Z_{a_E}(t)\right]_{\min} \le \Delta Z_E(t) \le \left[\Delta Z_{a_E}(t)\right]_{\max} \tag{48}$$

where

$$\left[\Delta Z_{a_E}(t)\right]_{\min} = \tau_E^2 \cdot [\psi(t_{\mathrm{go}}/\tau_E) + \mathrm{III}_E(t_f, t)] \cdot \left[x_4(t - \Delta t_{\mathrm{est}})e^{-\Delta t_{\mathrm{est}}/\tau_E} - a_E^{\max}\left(1 - e^{-\Delta t_{\mathrm{est}}/\tau_E}\right)\right] \tag{49}$$

$$\left[\Delta Z_{a_E}(t)\right]_{\max} = \tau_E^2 \cdot [\psi(t_{\mathrm{go}}/\tau_E) + \mathrm{III}_E(t_f, t)] \cdot \left[x_4(t - \Delta t_{\mathrm{est}})e^{-\Delta t_{\mathrm{est}}/\tau_E} + a_E^{\max}\left(1 - e^{-\Delta t_{\mathrm{est}}/\tau_E}\right)\right] \tag{50}$$

This uncertainty region in Z is shown in Fig. 5 for a case where without delay both $(t_{\mathrm{go}})_s$ and J_0^* are zero.

Based on an approach suggested by Petrosjan,[22] applied in a recent paper,[16] the reachable set of the evader has to be computed, and the pursuer should aim to the center of the convex hull of this reachable set. Using this approach results with a solution structure that is similar to the one depicted in Fig. 4 with the optimal strategies in region $\mathcal{D}_1$ being

$$u^* = v^* = \mathrm{sign}\{Z(t)_{\mathrm{av}}\}, \qquad \{Z(t)_{\mathrm{av}}\} \neq 0 \tag{51}$$

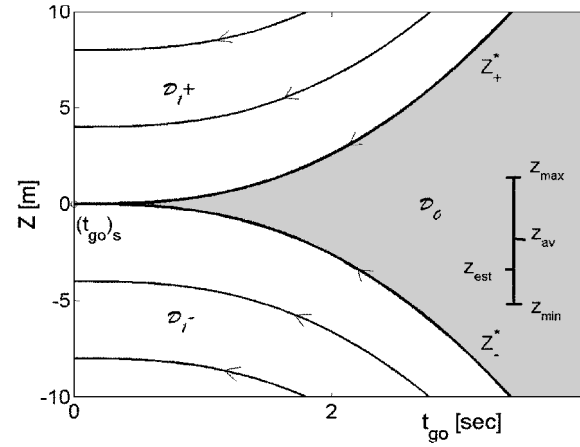

Fig. 5 Uncertainty bounds of Z.

where

$$Z(t)_{\mathrm{av}} = \{[Z(t)]_{\max} + [Z(t)]_{\min}\}/2 = Z_{\mathrm{PN}}(t) - \Delta Z_{a_p}(t) - \Delta Z_{\phi_p}(t) + \Delta Z_{\phi_E}(t) + \Delta Z_{a_E}^c(t) \tag{52}$$

and

$$\Delta Z_{a_E}^c(t) = x_4(t - \Delta t_{\mathrm{est}})e^{-\Delta t_{\mathrm{est}}/\tau_E}\tau_E^2 \cdot [\psi(t_{\mathrm{go}}/\tau_E) + \mathrm{III}_E(t_f, t)] \tag{53}$$

The line $Z(t)_{\mathrm{av}} = 0$ in region $\mathcal{D}_1$ is a dispersal surface dominated by the evader and hence $u^* = 0$ and $v^* = \pm 1$. As in the preceding section in region $\mathcal{D}_0$, the optimal strategies are arbitrary. Note that because of the estimation delay the values of $(t_{\mathrm{go}})_s$ and J_0^*, depending on the game parameters, are never zero. The control strategy of the pursuer, defined in Eq. (51), is adopted as a new interceptor guidance law. This new guidance law, integrating the elements of a time-varying linear model and the delay compensation, is denoted in the sequel as DGL/EC.

V. Outline of Three-Dimensional Estimator

For the implementation of the guidance law in a three-dimensional noise-corrupted environment, the estimator of Ref. 17 is selected. The estimator was derived in a rotating sensor frame assuming a high measurement rate and small angular deviations from the sensor boresight during target tracking. The measurements are range, azimuth, and elevation in the sensor frame and also the angular velocity of the frame. The resulting three-dimensional estimator consists of three independent filters, whose states are the relative position, relative velocity, and the target absolute acceleration along each sensor axis. The target models in each axis are also independent and identical. The rotation of the sensor frame is taken into account by using the instantaneously frozen coordinate system approach.

The coordinate system attached to the sensor is illustrated in Fig. 6. The range r and the angular deviations from the sensor boresight (the azimuth ϕ_{az} and the elevation ϕ_{el}) are also presented.

The state vector of each (single axis) filter is

$$\boldsymbol{W}^i = [p_i, v_i, a_{Ei}]^T, \qquad i = x, y, z \tag{54}$$

where p_i and v_i are the relative position and velocity, respectively. Using Eq. (54), a state matrix can be defined as

$$\boldsymbol{W} = \begin{bmatrix} (\boldsymbol{W}^x)^T \\ (\boldsymbol{W}^y)^T \\ (\boldsymbol{W}^z)^T \end{bmatrix} = \begin{bmatrix} p_x & v_x & a_{\mathrm{Ex}} \\ p_y & v_y & a_{\mathrm{Ey}} \\ p_z & v_z & a_{\mathrm{Ez}} \end{bmatrix} \tag{55}$$

The estimator uses the same dynamic model for the equations of motion in each of the instantaneously frozen sensor frame axes. Using the ECA/SF, the equations of a single-axis filter model are

$$\dot{\boldsymbol{W}}^i = \boldsymbol{A}_w \boldsymbol{W}^i + \boldsymbol{B}_w a_P + \boldsymbol{C}_w w$$
$$\boldsymbol{W}^i(0) = \boldsymbol{W}_0^i, \qquad i = x, y, z \tag{56}$$

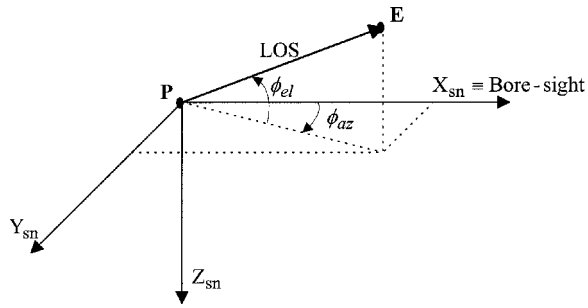

Fig. 6 Rotating sensor coordinate system used for target state estimation.

where

$$\boldsymbol{A}_w = \begin{bmatrix} 0 & 1 & 0 \\ 0 & 0 & 1 \\ 0 & 0 & -1/\tau_a \end{bmatrix} \tag{57}$$

$$\boldsymbol{B}_w = [0 \quad -1 \quad 0]^T \tag{58}$$

$$\boldsymbol{C}_w = [0 \quad 0 \quad 1]^T \tag{59}$$

and

$$w \sim WN(0, q), \qquad q(t) = \left[a_E^{\max}(t)\right]^2 \big/ 4 \tag{60}$$

In this ECA/SF the parameter τ_a is the assumed average time between the changes in the piecewise constant target acceleration levels. The value of $a_E^{\max}(t)$ is approximated online based on nominal trajectory data. If only a bound on the maximum acceleration of the evader is known, then this value should be used instead.

The sensor measurements are assumed to be

$$\boldsymbol{z} = \begin{bmatrix} r \\ \phi_{\text{az}} \\ \phi_{\text{el}} \end{bmatrix} + \boldsymbol{v} \cong \begin{bmatrix} \boldsymbol{H}^x \boldsymbol{W}^x \\ \boldsymbol{H}^y \boldsymbol{W}^y \\ \boldsymbol{H}^z \boldsymbol{W}^z \end{bmatrix} + \boldsymbol{v} \tag{61}$$

where

$$\boldsymbol{H}^x = [1 \quad 0 \quad 0] \tag{62}$$

$$\boldsymbol{H}^y = [1/\hat{r} \quad 0 \quad 0] \tag{63}$$

$$\boldsymbol{H}^z = [-1/\hat{r} \quad 0 \quad 0] \tag{64}$$

$$\boldsymbol{v} = [v_r, v_{\text{az}}, v_{\text{el}}], \qquad E(\boldsymbol{v}) = 0$$

$$E(\boldsymbol{v}\boldsymbol{v}^T) = \text{diag}\left[\sigma_r^2 \quad \sigma_{\text{az}}^2 \quad \sigma_{\text{el}}^2\right] \tag{65}$$

and $\hat{r}$ is the estimated range.

The discrete time version of the estimator equations is given in the Appendix for the sake of completeness.

VI. Simulation Study

In this section the validity of the integrated estimator–guidance law is tested using a modular three-dimensional nonlinear point–mass simulation of a ballistic missile defense scenario against a highly maneuvering TBM.

A. Monte Carlo Simulation

The simulation program includes the following elements: three-dimensional nonlinear relative kinematics between two point–mass vehicles, point–mass dynamics, and first-order control dynamics of each flying vehicle, a three-dimensional estimator (outlined in the preceding section) with a measurement frequency of 200 Hz and a high-altitude standard atmospheric model. The simulations were carried out in a fixed Cartesian coordinate system, assuming flat nonrotating Earth and no wind, using the well-known equations of three-dimensional kinematics as in Ref. 3. For each test point 100 simulations with different noise samples were used. The main parameters of the Monte Carlo simulation runs are summarized in Table 1.

Table 1 Simulation parameters

Evader	Pursuer	Estimation
$\tau_E = 0.2$ s	$\tau_P = 0.2$ s	$\tau_a = 1.5$ s
$a_{Ef}^{\max} = 21.5$ g	$a_{\text{Pf}}^{\max} = 48.4$ g	$\sigma_r = 0.1$ m
$V_{\text{Ef}} = 2.58$ km/s	$V_{\text{Pf}} = 3.17$ km/s	$\sigma_{\text{el}} = 0.1$ mrd
$\phi_E(0) = 0$ deg	$\phi_P(0) = 0$ deg	$\sigma_{\text{az}} = 0.1$ mrad

[a]Subscript f stands for the final value.

B. Maneuvering End Game

The presented results concentrate on the end game of the interception, where a sequence of two "hard" TBM maneuvers is assumed to take place. This end game starts when the TBM crosses the altitude of 28 km (with a flight path angle of 45 deg) and has a duration of 2.6 s. The initial TBM maneuver is commanded to a direction (either right or left) perpendicular to the vertical reference plane of the nominal trajectory. The sequence is completed by a second maneuver, commanded to the opposite direction, after some time t_{sw}. The values of t_{sw} vary between different simulation runs in small steps in the interval of $0 \le t_{\text{sw}} \le 2.6$ s. Actually, steps of 700 m of range, which correspond approximately to time steps of the order of 0.14 s, have been taken. The family of such end-game maneuver sequences with varying t_{sw} adequately represents the ensemble of the random maneuver samples that can be implemented by the designer of a TBM without the knowledge of the interception altitude.

C. Performance Index

In this simulation study with noisy measurements, the cost function of the perfect information game (the deterministic miss distance) is of no meaning. The outcome of a set of Monte Carlo simulations with random noise samples is the miss distance distribution. In reality, the objective of the interceptor designer is to guarantee the destruction of the incoming target with a predetermined probability of success, using the smallest possible warhead lethal radius R_k. In this study the required probability of success is assumed to be 0.95 against the worst feasible target maneuver. This probability is denoted as the single-shot kill probability[23] defined by

$$\text{SSKP} = \text{E}\{P_d(R_k)\} \tag{66}$$

where E is the mathematical expectation taken over the entire set of noise samples against any given feasible target maneuver and the simplified lethality function P_d is

$$P_d = \begin{cases} 1 & M \le R_k \\ 0 & M > R_k \end{cases} \tag{67}$$

where M is the miss distance.

D. Filter Performance

Figure 7 presents the estimation of the target horizontal acceleration. Even though the normalized acceleration command is of a bang-bang type, the command itself is time dependent because of the time-varying maximum acceleration. In the case of noise-free measurements, the output is almost identical to the ensemble average of the Monte Carlo runs with different noise samples and same timing of evader's acceleration switch [$(t_{\text{go}})_{\text{sw}} = 0.7$ s]. A small bias and an estimation delay of approximately $\Delta t_{\text{est}} = 0.15$ s, corresponding well to the precomputed detection time of $T_{\text{id}}^{\min}(r = 4\text{ km}) \cong 0.14$ s, are also apparent. The standard deviation computed from Monte Carlo runs corresponds to that of the filter.

Remark: The implemented estimator is by no means optimal; for example in an earlier two-dimensional study,[24] an efficient multiple model adaptive estimator, tailored to the discussed target maneuver strategy, was used with some homing improvement. Nonetheless, the simple estimator used here serves well for the guidance law performance comparison presented in the sequel.

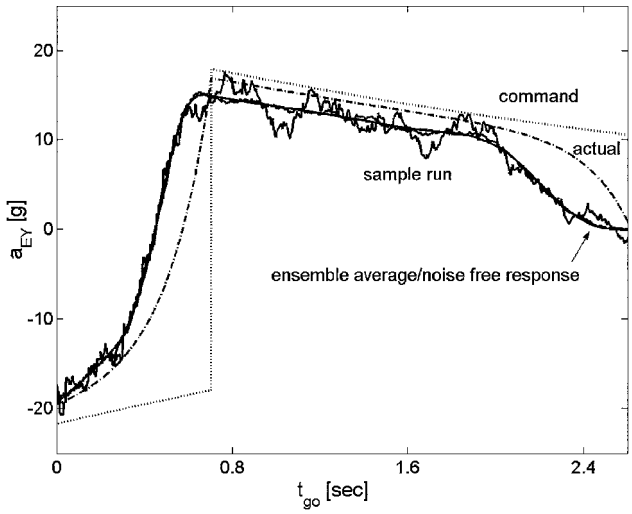

Fig. 7 Estimation of the target horizontal acceleration.

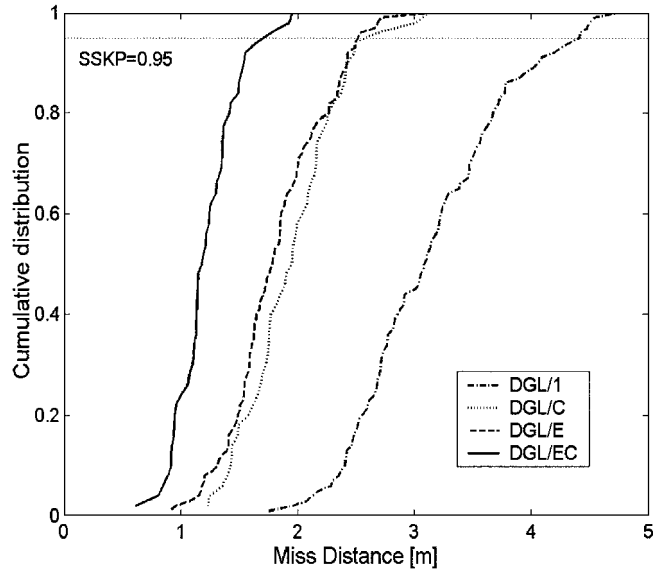

Fig. 8 Cumulative miss-distance distribution comparison.

E. Guidance Laws Implementation

Four different guidance laws, all having the form of Eqs. (51) and (52) but derived using different assumptions, were tested by the Monte Carlo simulations and compared: 1) DGL/1—perfect information ($\Delta t_{\text{est}} = 0$), constant velocities, and maneuverabilities[8]; 2) DGL/E—perfect information, linearly varying interceptor velocity, and target maneuverability[10]; 3) DGL/C—delayed information ($\Delta t_{\text{est}} \neq 0$), constant velocities, and maneuverabilities[16]; and 4) DGL/EC—delayed information, linearly varying interceptor velocity, and target maneuverability.

Remark:

1) In the implementation the estimated ZEM of each guidance law is used instead of the actual one. Because the boundary trajectories (Z_+^* and Z_-^*) separating the two regions of the game ($\mathcal{D}_0$ and $\mathcal{D}_1$) cannot be accurately known because of errors in estimating t_{go} and the maximum accelerations of both players as a result of the noisy measurements, the bang-bang strategy, optimal in both regions, is used.

2) The actual velocity profiles of both players are needed explicitly in the computation of the ZEM of DGL/E and DGL/EC and implicitly, via the computation of t_{go}, for all four guidance laws. In an actual implementation these profiles are unknown a priori; hence, the profiles on the nominal interception trajectory should be taken instead. The nominal trajectories of the interceptor and target missiles can be updated online during the engagement based on the information from the inertial measurement unit (IMU) and the target state estimator, respectively. In this study, based on Fig. 1, it was approximated (for the sake of a simple implementation) that the interceptor has a constant longitudinal acceleration and the reentry vehicle has a constant velocity.

F. Homing Performance

Because the maneuvers of the TBM are expected to be of a randomly switched bang-bang type, the worst timing for the maneuver switch has to be identified. The worst timing, different for each guidance law, is defined as the one corresponding to the target maneuver that requires the largest kill radius of the interceptor warhead for an SSKP of 0.95. In Fig. 8 the homing performance of the four different guidance laws is compared using the accumulated miss distance distributions for the worst target maneuver of each guidance law.

By using DGL/1 the actual miss distances are substantially larger than the zero miss distance predicted by the perfect information game solution with a constant speed model,[8] and the SSKP of 0.95 can be guaranteed only if the lethal radius of the warhead exceeds 4.4 m.

By applying DGL/C, which compensates for the estimation delay, the miss distances are substantially reduced, and the required SSKP of 0.95 can be guaranteed with a lethal radius of about 2.5 m. DGL/E, which models the time-varying velocities and maneuverabilities (but without delay compensation), provides a similar improvement.

By using the new guidance law derived in Sec. IV (DGL/EC), which integrates both of these elements, the miss distances are further reduced, and the SSKP of 0.95 can be guaranteed with a lethal radius of less then 1.7 m.

The constant estimation delay used in DGL/E and DGL/EC was selected as 0.1 s after a minmax search for the delay providing the best homing performance.

VII. Conclusions

A new guidance law was synthesized by integrating an estimation-delay model and a linear time-varying differential game formulation of an end-game interception scenario. The resulting deterministic guidance law was implemented in a realistic ballistic missile defense scenario with noisy measurements by using a suitable three-dimensional estimator. Testing this estimator/guidance algorithm in a generic (yet realistic) nonlinear, measurement noise-corrupted interception scenario against a highly maneuvering reentering tactical ballistic missile confirmed the validity of the research concept by demonstrating a substantial improvement in homing performance compared to earlier suggested guidance laws.

The new improved guidance law can be easily adopted in any existing (or currently developed) missile defense system because its implementation does not require any hardware modification. The demonstrated improved homing performance and the generic nature of the integrated estimator/guidance algorithm raise the justified hope that by its application the challenging (and not yet addressed) task of intercepting highly maneuvering vehicles, expected in future missile defense scenarios, can be successfully accomplished.

Appendix: Equations of the Discretized Estimator

Discrete Time Equations

The discrete time version of Eqs. (56–59) is

$$\boldsymbol{W}^i_{k+1} = \boldsymbol{F}\boldsymbol{W}^i_k + \boldsymbol{\Gamma} a^i_{pk} + \boldsymbol{G} w_k, \qquad i = x, y, z \tag{A1}$$

where $\boldsymbol{F}$, $\boldsymbol{\Gamma}$, and $\boldsymbol{G}$ are the discretized version of $\boldsymbol{A}_w$, $\boldsymbol{B}_w$, and $\boldsymbol{C}_w$, given in Eq. (57–59), respectively. The discrete noise is

$$w_k \sim WN(0, q_k), \qquad q_k = Tq \tag{A2}$$

where T is the sampling period.

Measurements Model

The sensor measurements are

$$z_k = \begin{bmatrix} r_k \\ (\phi_{\text{az}})_k \\ (\phi_{\text{el}})_k \end{bmatrix} + \boldsymbol{v} \cong \begin{bmatrix} \boldsymbol{H}^x_k \boldsymbol{W}^x_k \\ \boldsymbol{H}^y_k \boldsymbol{W}^y_k \\ \boldsymbol{H}^z_k \boldsymbol{W}^z_k \end{bmatrix} + \boldsymbol{v} \tag{A3}$$

where

$$\boldsymbol{H}_k^x = [1 \quad 0 \quad 0] \tag{A4}$$

$$\boldsymbol{H}_k^y = [1/\hat{r}_{k/k-1} \quad 0 \quad 0] \tag{A5}$$

$$\boldsymbol{H}_k^z = [-1/\hat{r}_{k/k-1} \quad 0 \quad 0] \tag{A6}$$

$$\boldsymbol{v} = [v_r, v_{\text{az}}, v_{\text{el}}], \qquad E(\boldsymbol{v}) = 0$$

$$E(\boldsymbol{v}\boldsymbol{v}^T) = \text{diag}\left[\sigma_r^2 \quad \sigma_{\text{az}}^2 \quad \sigma_{\text{el}}^2\right] \tag{A7}$$

Because the angular deviations ϕ_{az} and ϕ_{el} are assumed to be small, the target coordinates in the sensor frame are

$$x_{\text{sn}} \cong r, \qquad y_{\text{sn}} \cong r\phi_{\text{az}}, \qquad z_{\text{sn}} \cong -r\phi_{\text{el}} \tag{A8}$$

It is assumed that the range measurement is quite accurate, and therefore

$$\sigma_{x_{\text{sn}}} \cong \sigma_r, \qquad \sigma_{y_{\text{sn}}} \cong r\sigma_{\text{az}}, \qquad \sigma_{z_{\text{sn}}} \cong r\sigma_{\text{el}} \tag{A9}$$

It is also assumed that the pursuer's own acceleration and the sensor frame angular velocity are accurately measured. These measurements can be performed by an IMU and rate gyros, respectively.

Three-Dimensional Filter Equations

Using the dynamic model of Eq. (A1), the measurement model of Eqs. (A3–A7), and the instantaneously frozen frame approach, a discrete Kalman filter is implemented.

The time update equations are

$$\hat{\boldsymbol{W}}_{k+1/k} = \boldsymbol{\Psi}_{k+1,k}\hat{\boldsymbol{W}}_{k/k}\boldsymbol{F}^T + \boldsymbol{U}_k \tag{A10}$$

$$\boldsymbol{P}^i_{k+1/k} = \boldsymbol{F}\boldsymbol{P}^i_{k/k}\boldsymbol{F}^T + \boldsymbol{Q}^i_k, \qquad i = x, y, z \tag{A11}$$

where the known variable $\boldsymbol{U}_k$ is defined by

$$\boldsymbol{U}_k = \left(a_P^i\right)_k \boldsymbol{\Gamma}^T, \qquad i = x, y, z \tag{A12}$$

and $\boldsymbol{\Psi}_{k+1,k}$ is the transformation from the sensor coordinate system at time k to the sensor coordinate system at time $k+1$ defined as

$$\boldsymbol{\Psi}_{k+1,k} = \begin{bmatrix} 1 & T\omega_{\text{zk}} & -T\omega_{\text{yk}} \\ -T\omega_{\text{zk}} & 1 & T\omega_{\text{xk}} \\ T\omega_{\text{yk}} & -T\omega_{\text{xk}} & 1 \end{bmatrix} \tag{A13}$$

where ω_k is the angular velocity of the sensor frame at time k, relative to an inertial frame and expressed in the sensor frame.

Assuming that 1) the sensor frame is roll stabilized and that 2) the sensor bore-sight coincides with $\hat{\text{LOS}}_k$ (the estimated line-of-sight direction at time k) during $t_k \le t \le t_{k+1}$ and jumps to $\hat{\text{LOS}}_{k+1}$ at time t_{k+1}, the matrix $\boldsymbol{\Psi}_{k+1,k}$ can be calculated as

$$\boldsymbol{\Psi}_{k+1,k} = \left.\begin{bmatrix} 1 & \hat{\phi}_{\text{az}} & -\hat{\phi}_{\text{el}} \\ -\hat{\phi}_{\text{az}} & 1 & 0 \\ \hat{\phi}_{\text{el}} & 0 & 1 \end{bmatrix}\right|_{k+1/k} \tag{A14}$$

Based on the assumption that the interceptor's own acceleration and the sensor frame angular velocity are known, the process noise covariance $\boldsymbol{Q}^i_k$ is reduced to

$$\boldsymbol{Q}^i_k = q_k \boldsymbol{G}\boldsymbol{G}^T \tag{A15}$$

The measurement update equations are

$$\hat{\boldsymbol{W}}_{k+1/k+1} = \hat{\boldsymbol{W}}_{k+1/k} + \Delta\boldsymbol{W}_{k+1} \tag{A16}$$

$$\boldsymbol{L}^i_{k+1} = \boldsymbol{P}^i_{k+1/k}\left(\boldsymbol{H}^i_{k+1}\right)^T\left(\boldsymbol{S}^i_{k+1}\right)^{-1}, \qquad i = x, y, z \tag{A17}$$

$$\boldsymbol{P}^i_{k+1/k+1} = \boldsymbol{M}^i_{k+1}\boldsymbol{P}^i_{k+1/k}\left(M^i_{k+1}\right)^T + \boldsymbol{L}^i_{k+1}\text{R}^i_{k+1}\left(\boldsymbol{L}^i_{k+1}\right)^T \qquad i = x, y, z \tag{A18}$$

where

$$\boldsymbol{M}^i_{k+1} = \boldsymbol{I}_3 - \boldsymbol{L}^i_{k+1}\boldsymbol{H}^i_{k+1}, \qquad i = x, y, z \tag{A19}$$

$$\Delta\boldsymbol{W}_{k+1} = \begin{bmatrix} \left(\boldsymbol{L}^x_{k+1}\right)^T\tilde{\boldsymbol{z}}_{k+1}(1) \\ \left(\boldsymbol{L}^y_{k+1}\right)^T\tilde{\boldsymbol{z}}_{k+1}(2) \\ \left(\boldsymbol{L}^z_{k+1}\right)^T\tilde{\boldsymbol{z}}_{k+1}(3) \end{bmatrix} \tag{A20}$$

$$\boldsymbol{S}^i_{k+1} = \boldsymbol{H}^i_{k+1}\boldsymbol{P}^i_{k+1/k}\left(\boldsymbol{H}^i_{k+1}\right)^T + R^i_{k+1}, \qquad i = x, y, z \tag{A21}$$

$$\tilde{\boldsymbol{z}}_{k+1} = \boldsymbol{z}_{k+1} - \hat{\boldsymbol{z}}_{k+1/k} \tag{A22}$$

and

$$\hat{z}_{k+1/k} = \begin{bmatrix} \hat{\boldsymbol{W}}_{k+1/k}(1,1) \\ \hat{\boldsymbol{W}}_{k+1/k}(2,1)/\hat{\boldsymbol{W}}_{k+1/k}(1,1) \\ -\hat{\boldsymbol{W}}_{k+1/k}(3,1)/\hat{\boldsymbol{W}}_{k+1/k}(1,1) \end{bmatrix} \tag{A23}$$

$$\text{R}^x_{k+1} = \left(\sigma_r^2\right)_{k+1}, \qquad \text{R}^y_{k+1} = \left(\sigma_{\text{az}}^2\right)_{k+1}$$

$$\text{R}^z_{k+1} = \left(\sigma_{\text{el}}^2\right)_{k+1} \tag{A24}$$

References

[1] Hughes, D., "Next Arrow Test This Summer After Scoring Direct Hit," *Aviation Week and Space Technology*, Vol. 146, No. 12, 1997, p. 34.

[2] Philips, H. E., "PAC-3 Missile Seeker Tests Succeed," *Aviation Week and Space Technology*, Vol. 150, No. 12, 1999, p. 30.

[3] Shinar, J., Shima, T., and Kebke, A., "On the Validity of Linearized Analysis in the Interception of Reentry Vehicles," *Proceedings of the AIAA Guidance, Navigation, and Control Conference*, AIAA, Reston, VA, 1998, pp. 1050–1060.

[4] Shinar, J., and Shima, T., "Guidance Law Evaluation in Highly Nonlinear Scenarios—Comparison to Linear Analysis," *Proceedings of the AIAA Guidance, Navigation, and Control Conference*, AIAA, Reston, VA, 1999, pp. 651–661.

[5] Zarchan, P., *Tactical and Strategic Missile Guidance*, Progress in Astronautics and Aeronautics, Vol. 176, AIAA, Reston, VA, 1997, pp. 143–161.

[6] Gutman, S., and Leitmann, G., "Optimal Strategies in the Neighborhood of a Collision Course," *AIAA Journal*, Vol. 14, No. 9, 1976, pp. 1210–1212.

[7] Gutman, S., "On Optimal Guidance for Homing Missiles," *Journal of Guidance and Control*, Vol. 3, No. 4, 1979, pp. 296–300.

[8] Shinar, J., "Solution Techniques for Realistic Pursuit-Evasion Games," *Advances in Control and Dynamic Systems*, Vol. 17, Academic Press, New York, 1981, pp. 63–124.

[9] Gazit, R., and Gutman, S., "Development of Guidance Laws for a Variable-Speed Missile," *Dynamics and Control*, Vol. 1, No. 2, 1991, pp. 177–198.

[10] Shima, T., and Shinar, J., "Time Varying Pursuit Evasion Game Models with Bounded Controls," *Journal of Guidance, Control, and Dynamics*, Vol. 25, No. 3, 2002, pp. 425–432.

[11] Bar-Shalom, Y., and Li, X. R., *Estimation and Tracking: Principles, Techniques, and Software*, Artech House, Boston, 1993, p. 262.

[12] Singer, R. A., "Estimating Optimal Tracking Filter Performance for Manned Maneuvering Targets," *IEEE Transactions on Aerospace and Electronic Systems*, Vol. AES-6, No. 4, 1970, pp. 473–483.

[13] Zarchan, P., "Representation of Realistic Evasive Maneuvers by the Use of Shaping Filters," *Journal of Guidance and Control*, Vol. 2, No. 4, 1979, pp. 290–295.

[14] Shinar, J., and Shima, T., "Robust Missile Guidance Law Against Highly Maneuvering Targets," *Proceedings of the 7th IEEE Mediterranean Conference on Control and Automation*, Inst. of Electrical and Electronics Engineers, New York, 1999, pp. 1548–1572.

[15] Witsenhausen, H. S., "Separation of Estimation and Control for Discrete Time Systems," *Proceedings of the IEEE*, Vol. 59, No. 11, 1971, pp. 1557–1566.

[16] Shinar, J., and Shima, T., "Non-Orthodox Guidance Law Development Approach for the Interception of Maneuvering Anti-Surface Missiles," *Journal of Guidance, Control, and Dynamics*, Vol. 25, No. 4, 2002, pp. 658–666.

[17]Weiss, H., and Hexner, G., "A Simple Structure for a High Performance 3-D Tracking Filter," Technion—Israel Inst. of Technology, Dept. of Aerospace Engineering, TAE Rept. 858, Haifa, Israel, Feb. 2001, pp. 15–23.

[18]Adler, F. P., "Missile Guidance by Three-Dimensional Proportional Navigation," *Journal of Applied Physics*, Vol. 27, No. 5, 1956, pp. 500–507.

[19]Forte, I., Steinberg, A., and Shinar, J., "The Effects of Non-Linear Kinematics in Optimal Evasion," *Optimal Control Application and Methods*, Vol. 4, No. 2, 1983, pp. 139–152.

[20]Shinar, J., Rotsztein, Y., and Bezner, A., "Analysis of Three-Dimensional Optimal Evasion with Linearized Kinematics," *Journal of Guidance and Control*, Vol. 2, No. 5, 1979, pp. 353–360.

[21]Hexner, G., Weiss, H., and Dror, S., "Temporal Multiple Model Estimator for a Maneuvering Target," Technion—Israel Inst. of Technology, Dept. of Aerospace Engineering, TAE Rept. 859, Haifa, Israel, Feb. 2001, pp. 23, 24.

[22]Petrosjan, L. A., *Differential Games of Pursuit*, Series on Optimization, Vol. 2, World Scientific, Singapore, 1993, pp. 169–177.

[23]Forte, I., and Shinar, J., "Improved Guidance Law Design Based on Mixed Strategy Concept," *Journal of Guidance, Control, and Dynamics*, Vol. 12, No. 5, 1989, pp. 739–745.

[24]Shima, T., Oshman, Y., and Shinar, J., "Efficient Multiple Model Adaptive Estimation in Ballistic Missile Interception Scenarios," *Journal of Guidance, Control, and Dynamics*, Vol. 25, No. 4, 2002, pp. 667–675.